

RAPID COMMUNICATION | FEBRUARY 09 2009

A one-dimensional free energy surface does not account for two-probe folding kinetics of protein α_3D **FREE**

Feng Liu; Charles Dumont; Yongjin Zhu; William F. DeGrado; Feng Gai; Martin Gruebele



J. Chem. Phys. 130, 061101 (2009)

<https://doi.org/10.1063/1.3077008>



Nanotechnology & Materials Science



Optics & Photonics



Impedance Analysis



Scanning Probe Microscopy



Sensors



Failure Analysis & Semiconductors



Unlock the Full Spectrum.
From DC to 8.5 GHz.

Your Application. Measured.

Find out more

Zurich Instruments

A one-dimensional free energy surface does not account for two-probe folding kinetics of protein α_3 D

Feng Liu,¹ Charles Dumont,² Yongjin Zhu,³ William F. DeGrado,⁴ Feng Gai,³ and Martin Gruebele^{1,2,5,a)}

¹Center for Biophysics and Computational Biology, University of Illinois at Urbana-Champaign, Illinois 61801, USA

²Department of Physics, University of Illinois at Urbana-Champaign, Illinois 61801, USA

³Department of Chemistry, University of Pennsylvania, Philadelphia, Pennsylvania 19104, USA

⁴Department of Biochemistry and Biophysics, University of Pennsylvania, Philadelphia, Pennsylvania 19104, USA

⁵Department of Chemistry, University of Illinois at Urbana-Champaign, Illinois 61801, USA

(Received 26 September 2008; accepted 9 December 2008; published online 9 February 2009)

We present fluorescence-detected measurements of the temperature-jump relaxation kinetics of the designed three-helix bundle protein α_3 D taken under solvent conditions identical to previous infrared-detected kinetics. The fluorescence-detected rate is similar to the IR-detected rate only at the lowest temperature where we could measure it (326 K). The fluorescence-detected rate decreases by a factor of 3 over the 326–344 K temperature range, whereas the IR-detected rate remains nearly constant over the same range. To investigate this probe dependence, we tested an extensive set of physically reasonable one-dimensional (1D) free energy surfaces by Langevin dynamics simulation. The simulations included coordinate- and temperature-dependent roughness, diffusion coefficients, and IR/fluorescence spectroscopic signatures. None of these can reproduce the IR and fluorescence data simultaneously, forcing us to the conclusion that a 1D free energy surface cannot accurately describe the folding of α_3 D. This supports the hypothesis that α_3 D has a multidimensional free energy surface conducive to downhill folding at 326 K, and that it is already an incipient downhill folder with probe-dependent kinetics near its melting point. © 2009 American Institute of Physics. [DOI: 10.1063/1.3077008]

I. INTRODUCTION

Protein folding is generally treated as an activated unimolecular reaction or as a sequence of such steps.¹ When compared to prefactors in the 0.1–10 μ s range,² typical reaction times in the millisecond to minute range justify the use of activation models such as Kramers' rate theory.^{3,4} For a single activation barrier, such models predict exponential two-state folding kinetics, in which all thermodynamic and kinetic observables switch from unfolded reactant to folded product in a synchronized manner.¹

During the past decade, it has become recognized theoretically,⁵ computationally,^{6–9} and experimentally^{10–15} that small proteins could fold much faster yet, approaching the downhill folding limit where the activation barrier becomes comparable to $k_B T$.^{16,17} Such efficiency is realized when short-range and long-range interactions within the protein and between protein and solvent harmonize en route to the native state ("consistency"¹⁸ and "minimal frustration"¹⁹ in the statistical mechanical literature). Proteins can also be poised at the transition state to fold downhill from there.²⁰ The experimental observation of downhill folding represents a major validation of theories and simulations invoking minimal frustration.

Two general methods have been used to identify down-

hill folding. In the thermodynamic approach, the temperature is tuned to identify probe-dependent denaturation base lines and melting temperatures. Those probes that switch signal at lower free energy yield lower melting temperatures.^{11,21–25} In the kinetic approach, the temperature is tuned to identify the appearance of probe-dependent rates and the appearance/disappearance of nonexponential kinetics.^{10,12,26,27} Generally, folding barriers ΔG^\ddagger decrease as we tune from the melting temperature T_m to the temperature of maximum stability. When $\Delta G^\ddagger > 3 k_B T$, activated kinetics with a single rate coefficient k_a are observed. When $\Delta G^\ddagger < 1 k_B T$, diffusive downhill dynamics characterized by a rate coefficient k_m are observed (assuming normal diffusion).^{23,28,29} At intermediate temperatures, nonexponential kinetics with both k_m and k_a are observed.¹⁷ Both thermodynamic and kinetic methods rely on tuning a thermodynamic parameter (e.g., T), not on a single-point measurement.³⁰

The designed protein α_3 D is a likely candidate for downhill folding. If pure downhill diffusion on the free energy surface of reaction is normal Stokes–Einstein diffusion, then exponential kinetics with a very fast rate coefficient k_m result.³¹ The infrared-detected folding kinetics of α_3 D are exponential, with a very fast observed rate coefficient $k_{\text{obs}} \approx (3 \mu\text{s})^{-1}$ that is nearly temperature independent between 318–345 K.²⁹

Multiple probes that switch signal at different places along the reaction coordinate could still lead to different ob-

^{a)}Author to whom correspondence should be addressed. Electronic mail: gruebele@scs.uiuc.edu.

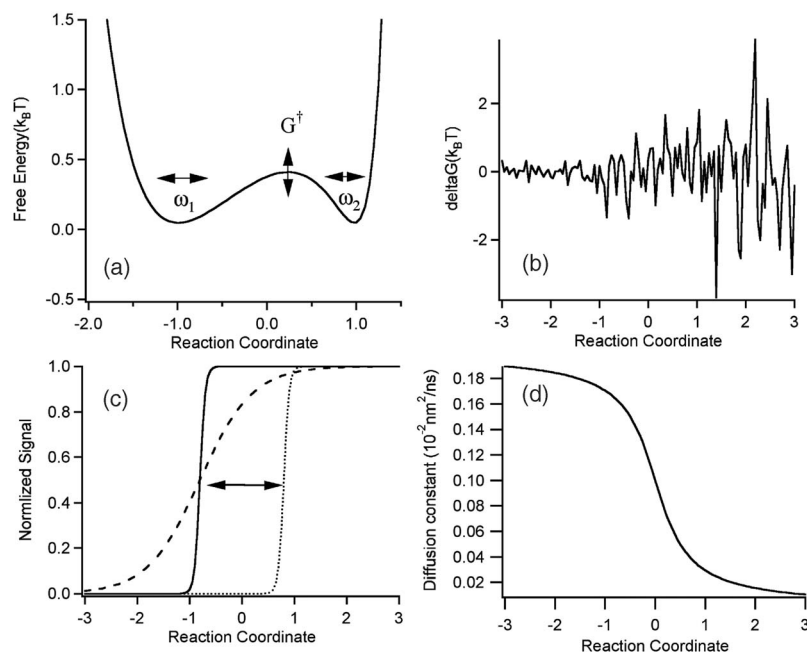


FIG. 1. Types of 1D free energy surfaces $G(x)$ (a), coordinate-dependent free energy roughness (b), coordinate-dependent probe functions $S(x)$ (c), and coordinate-dependent diffusion coefficients $D(x)$ (d) tested by LD in 1D.

served relaxation times, particularly if destabilizing the protein near its melting temperature turns it from a downhill folder into an incipient downhill folder. Therefore we investigate α_3D by measuring the folding-induced fluorescence lifetime shift and compare it with the infrared results. Unlike IR detection, which yields a nearly constant rate coefficient over the temperature range probed here,²⁹ fluorescence detection shows a factor of 3 decrease in the rate coefficient as the temperature is raised from 326 to 344 K. This observation is not compatible with an activated two-state model, but the discrepancy is large enough that we can go a step further in the analysis,

We conclude that the data cannot be accounted for by physically reasonable one-dimensional (1D) free energy models. Even downhill folders are usually approximately accounted for by 1D free energy surfaces with very low barriers,^{12,28} although in one case a better fit to the data was obtained with a two-dimensional (2D) surface.²⁶ Here we systematically consider coordinate-dependent probes, coordinate-dependent roughness or diffusion coefficients, and many shapes of high- and low-barrier surfaces to attempt to fit the IR and fluorescence data simultaneously. Even physically unlikely model variations cannot account for the data quantitatively. The key problem is that fluorescence-detected observed rates are slower than IR-detected kinetics at high temperature, yet the latter remain exponential with very good signal to noise ratio.

α_3D will require a 2D free energy surface to explain the temperature dependence of the observed rate coefficients measured by two probes. Addition of further probes may require even more reaction coordinates, although we expect that additional probes eventually become linearly dependent on one another, capping the number of required coordinates.

II. METHODS

α_3D is a *de novo* designed 73-residue three-helix bundle protein (PDB ID 2A3D).³² To make a direct comparison with

the folding kinetics measurement monitored by infrared absorption spectroscopy of the amide I' band at 1631 and 1665 cm^{-1} ,²⁹ the protein sample was purified and prepared in the same way as described in Ref. 29. Thermal denaturation of α_3D was carried out on a Jasco J-715 equipped with a Peltier temperature control (Jasco) by monitoring circular dichroism (CD) at 222 nm and integrated fluorescence excited at 280 and 295 nm simultaneously. Protein folding kinetics were measured with a laser-induced temperature jump setup by detecting a tryptophan fluorescence signal excited at 280 nm.³³ The temperature jump size ranged from 8–10 K and the final temperature after T-jump spanned the range from 326 to 344 K (nearly up to the protein melting temperature). Tryptophan fluorescence decays were recorded every 14 ns for up to 500 μs and with 500 ps time resolution. With

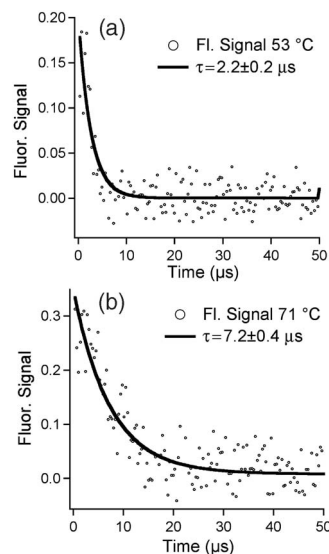


FIG. 2. Example of the fluorescence-detected kinetics data obtained at low temperature (a) and high temperature (b). The IR-detected kinetics do not show a similar slow down (Ref. 29). The curves going through the data points are single exponential fits of the observed rate coefficient k_{obs} .

χ analysis,³⁴ the kinetics of relaxation upon temperature jump are revealed by the evolution of the fluorescence lifetime profile change toward the higher temperature equilibrium. Due to the beginning of laser-induced cavitation and a decrease in the fluorescence signal above 344 K, we were not able to obtain reliable fluorescence data at higher temperatures.

We performed Langevin dynamics (LD) simulations on 1D free energy surfaces to investigate the folding kinetics of α_3 D observed with both IR and fluorescence probes. The details of the LD simulation, as we have implemented it, are described in Ref. 35. Briefly, LD in the high friction limit are used to obtain the relaxation of $\rho(x, t)$, the population distribution along the reaction coordinate, from the initial equilibrium to the new equilibrium after the free energy surface is perturbed by a T-jump at $t=0$. Given a specific dependence $S_P(x-x_P)$ of the probe signal along the reaction coordinate [Fig. 1(c)], the observed IR or fluorescence signal can be generated by integrating

$$S_P(t) = \int dx S_P(x - x_P) \rho(x, t). \quad (1)$$

The subscript P in Eq. (1) indicates either IR or fl (=fluorescence). LD simulations on low barrier 1D or 2D surfaces have been demonstrated to reproduce the kinetics of many fast folders, including single- and double-exponential kinetics and probe-dependent kinetics.³⁶ Here we systematically varied the key building blocks of the 1D free energy surface related to α_3 D kinetics (Fig. 1). By changing ΔG^\ddagger , the barrier height, between 0 and $3 k_B T$ and by varying ω_1 and ω_2 , the curvatures of the unfolded and native wells, free energy surfaces with different shapes can be generated. When $\Delta G^\ddagger=0$ and $\omega_1=\omega_2$, the double well free energy surface converges to a single well free energy surface. S was varied to switch at different x_P and given different x and T dependences. Coordinate-dependent roughness and diffusion constants³⁷ were also tested to fit the observed folding kinetics (see Supplement for explicit functional forms of surfaces, probe signals, roughness, and diffusion constants³⁸).

III. RESULTS

The observed fluorescence-detected kinetics traces could be fitted to single exponential decays within the experimental signal to noise ratio (Fig. 2). The observed relaxation time τ_{obs} has significant temperature dependence over the range from 326 to 344 K (Fig. 3). τ_{obs} is only 2.2 μs at 326 K and increases to 7.2 μs when the temperature is raised to 344 K (Fig. 2). In contrast, the observed IR relaxation time changes very little from 2.8 μs at 327 K to 2.6 μs at 344 K.²⁹ The IR-detected kinetics also remain exponential. The Arrhenius plots of the observed rate coefficients probed by IR and fluorescence converge only at the lowest temperatures (Fig. 3). At the highest temperature of 344 K, just below the melting transition midpoint, the IR-probed folding rate is about three times faster than the fluorescence probed folding rate. Such probe-dependent kinetics is clearly different from two-state

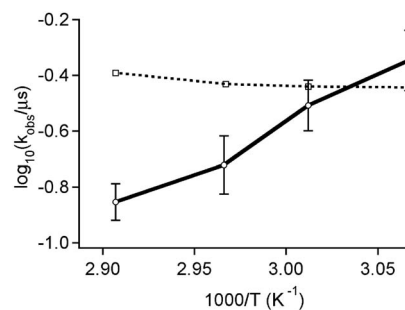


FIG. 3. Comparison of fluorescence-detected observed rate coefficients (\circ) with infrared-detected kinetics (\square) from Ref. 29.

folding kinetics, ruling out a high-barrier double well surface with spectroscopic signatures $S(x-x_P)$ switching near the transition state.³⁵

We tested a full range of 1D low barrier free energy surfaces by systematically varying the parameters illustrated in Fig. 1 (equations are given in Supplement³⁸). We failed to find a set of parameters that accounts for both the IR and fluorescence probed kinetics simultaneously over the measured temperature range.

The closest fit to experimental data is a double-well scenario with a barrier of only $1 k_B T$ at low temperature and $<3 k_B T$ near the melting point (see Supplement for functional form³⁸). The folding kinetics in this scenario strongly depend on the switching position x_P and on the shape of the probe function $S_P(x-x_P)$. Only when the switching position x_{IR} is close to 0 do we simulate single exponential kinetics in accordance with the excellent signal-to-noise ratio of the IR experiment. However, if x_{IR} is approximately set to 0 for the IR signal, no probe function $S_{\text{fl}}(x-x_{\text{fl}})$ can be found to represent the fluorescence probed kinetics accurately. As shown in Fig. 4, we can tune the calculated fluorescence signal from

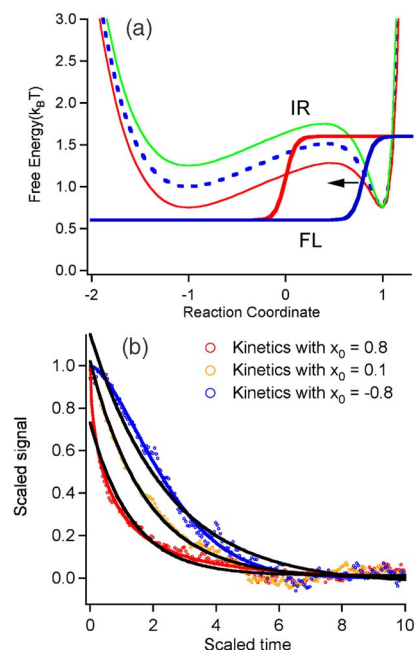


FIG. 4. (Color online) Best case LD simulations showing that quantitative agreement with both experimental probes (b) cannot be obtained simultaneously by us using a 1D free energy surface (a).

faster than the IR signal at low temperature to slower than the IR signal at high temperature, if x_{fl} is allowed to sweep all the way from the native state to the unfolded state with increasing temperature. However, we cannot reproduce the observed $>300\%$ change in the rate. The calculated range is off by more than a factor of 7 from experiment. Furthermore we need to move x_{fl} so close to the native or unfolded minima that major deviations from single exponential relaxation occur, outside even the larger measurement uncertainty of the fluorescence data. Although the single well scenario yielded observed kinetics that could be fitted to single exponential decays, the observed rate from different probe functions is still too weakly temperature dependent.

We also tested the effect of a coordinate-dependent diffusion constant D or roughness (Fig. 1) to increase rate variation. Again, the difference of the rates produced by different probe functions S is smaller than the difference of the rates observed by IR and fluorescence at high temperature for surfaces compatible with equilibrium titration data. To still yield accurate equilibrium properties for $\alpha_3\text{D}$, drastic variations in D or roughness along x required adjustments of the free energy profile that compensated for any increase in the calculated rate variation.

Thus the experiments and simulations show that $\alpha_3\text{D}$ is not a two state folder with a $>3 k_B T$ barrier, not even near its melting temperature, and that its low-barrier dynamics cannot be described by a 1D free energy surface.

IV. DISCUSSION

When the folding barrier height of a protein approaches $k_B T$, there is no well-defined native and unfolded state because all the subpopulations along the reaction coordinates are in rapid exchange. As a result, observed kinetic or thermodynamic signals are very sensitive to the probe used. Several incipient downhill or downhill protein folders, such as Trpzip2, B domain of protein A, and a mutant of lambda repressor YA (Q33YY22WG4648A), have such probe-dependent kinetics.^{35,39,40} In addition BBL, trpzip2, the lambda repressor mutant HG (Q33HY22WA3749G), and gpW have probe-dependent thermodynamics.^{8,11,23,25}

Fluorescence probes primarily the local solvation environment around the tryptophan residue, while IR probes backbone hydrogen bonding within the helices, but also loop hydrogen bonding. The two probes are thus sensitive to distinctly different parts of the protein environment.

The observed folding rate is similar by IR and fluorescence at low temperature, where the protein is most stable. The observed values of 2.2–2.6 μs are very close to its folding speed limit.¹⁶ If we assume the prefactor obeys Eaton's empirical folding limit for a 73-residue protein, i.e., $73/100=0.73 \mu\text{s}$,¹⁶ then the folding barrier probed by IR is about $1.5 k_B T (k_B T \ln[0.73k_f])$ at 327 K, and about $1 k_B T$ by fluorescence at 326 K. At higher temperature, the kinetics becomes probe dependent. The folding barrier probed by fluorescence increases from 1 to $3 k_B T$ as temperature is increased over the measured range. If $\alpha_3\text{D}$ is an incipient downhill folder at higher temperature, then the fluorescence-detected kinetics monitors a combination of k_a and k_m , and

the IR-detected kinetics monitors predominantly the molecular diffusion rate k_m . Interestingly, the folding barrier of $\alpha_3\text{D}$ was predicted to be less than $1 k_B T$ by a 1D free energy surface model fitted just to the IR data, in agreement with what we find here.⁴¹

The observed probe dependence could not be reproduced by us with LD simulations on any 1D free energy surface. 1D surfaces have worked well for most peptides and proteins reported,^{12,28,36,42} except in one published case (the incipient downhill folder $\lambda_{6-85}\text{YA}$).²⁶ The folding kinetics of $\alpha_3\text{D}$ probed by IR and fluorescence are another exception. All the physically reasonable (and unreasonable) 1D free energy surfaces we tested failed to reproduce the temperature- and probe-dependent kinetics of $\alpha_3\text{D}$.

The fitting problem could be clearly eliminated by using a 2D surface because only two probes have been observed so far. The data would not uniquely constrain such a surface, but the surface would have to have the following properties. Along the reaction coordinate corresponding to secondary structure formation probed by IR, the free energy surface has very small barriers $\leq 1.5 k_B T$; fast IR signals imply efficient loop and helix formation. Along the reaction coordinate corresponding to the tertiary structure formation probed by tryptophan fluorescence, the projected free energy surface is a double well separated by a small barrier whose height increases from 1.5 to $3 k_B T$ between 326 and 344 K. The probe surfaces $S_{\text{fl}}(x_{\text{fl}}, x_{\text{IR}})$ and $S_{\text{IR}}(x_{\text{fl}}, x_{\text{IR}})$ would be roughly orthogonal in this model.

We also observed the melting temperatures of $\alpha_3\text{D}$ monitored by five different probes (IR, CD, and integrated fluorescence intensity at different wavelengths, see Supplement). The deviation of T_m was ± 2 K, slightly larger than the temperature measurement uncertainty of ± 1 K. As a caveat, the high temperature baselines could not be recorded reliably because of the high melting temperature of $\alpha_3\text{D}$, but slightly probe-dependent thermodynamics of $\alpha_3\text{D}$ could be another indication that $\alpha_3\text{D}$ is an incipient downhill folder (barrier $\leq 3 k_B T$) at its melting temperature.

The low barrier of $\alpha_3\text{D}$ probably results from its computational design lacking evolutionary pressure. $\alpha_3\text{D}$ shows most hallmarks of native proteins, but it is an early computational design, and it has been suggested that $\alpha_3\text{D}$ has a more malleable and flexible hydrophobic core than most evolved native proteins.³² The flexibility of the hydrophobic core of $\alpha_3\text{D}$ lies between that of a native protein and a molten globule.³² By lowering the pH of the protein solution from 5.0 (Ref. 32) to 2.6 (present work and IR study²⁹), the flexibility of the hydrophobic core of $\alpha_3\text{D}$ could be tuned to be even more molten globule-like.

Several experimental observations support the connection between a less tightly packed hydrophobic core and downhill folding. Downhill folding was first used to explain the formation of a molten globule of phosphoglycerate kinase.¹⁰ Other downhill folders that fold downhill even at their T_m are either engineered proteins with weaker hydrophobic cores (protein Lambda repressor HG)²⁵ or natural proteins with loosely packed hydrophobic cores (BBL and gpW).^{11,23} $\alpha_3\text{D}$ itself has a somewhat lower heat capacity for folding than the average for natural proteins, indicative of

slightly greater penetration of water molecules in the native state,⁴³ and the designed protein was more forgiving of core mutations than for most natural proteins.⁴⁴ All of these observations taken together strongly suggest that the reduced desolvation barrier and reduced frustration of less packed hydrophobic cores play important roles in facilitating downhill folding.

With its very fast and probe-dependent folding kinetics, α_3 D will be an excellent model protein to test molecular dynamics simulations using hydrogen bonding (IR) and tryptophan flexibility and burial (fluorescence) as computational coordinates. Very different temperature dependence of kinetics observed by several probes that are at least partly complementary will require higher-dimensional free energy surfaces with different profiles and/or diffusion properties along different reaction coordinates.

ACKNOWLEDGMENTS

This work was funded by grants NSF MCB (Grant No. 0613643) (M.G.) and NIH (Grant No. GM-065978) (F.G.).

¹ *Protein Folding Handbook*, edited by J. Buchner and T. Kiefhaber (Wiley, New York, 2005).

² S. J. Hagen, J. Hofrichter, and W. A. Eaton, *J. Phys. Chem. B* **101**, 2352 (1997).

³ H. A. Kramers, *Physica* **7**, 284 (1940).

⁴ D. K. Klimov and D. Thirumalai, *Phys. Rev. Lett.* **79**, 317 (1997).

⁵ J. D. Bryngelson, J. N. Onuchic, N. D. Socci, and P. G. Wolynes, *Proteins* **21**, 167 (1995).

⁶ T. V. Pogorelov and Z. Luthey-Schulten, *Biophys. J.* **87**, 207 (2004).

⁷ S. S. Cho, P. Weinkam, and P. G. Wolynes, *Proc. Natl. Acad. Sci. U.S.A.* **105**, 118 (2008).

⁸ W. Y. Yang, J. Pitera, W. Swope, and M. Gruebele, *J. Mol. Biol.* **336**, 241 (2004).

⁹ J. W. Pitera, W. C. Swope, and F. F. Abraham, *Biophys. J.* **94**, 4837 (2008).

¹⁰ J. Sabelko, J. Ervin, and M. Gruebele, *Proc. Natl. Acad. Sci. U.S.A.* **96**, 6031 (1999).

¹¹ M. Garcia-Mira, M. Sadqi, N. Fischer, J. M. Sanchez-Ruiz, and V. Muñoz, *Science* **298**, 2191 (2002).

¹² W. Y. Yang and M. Gruebele, *Nature (London)* **423**, 193 (2003).

¹³ M. J. Parker and S. Marqusee, *J. Mol. Biol.* **293**, 1195 (1999).

¹⁴ D. T. Leeson, F. Gai, H. M. Rodriguez, L. M. Gregoret, and R. B. Dyer,

Proc. Natl. Acad. Sci. U.S.A. **97**, 2527 (2000).

¹⁵ J. B. Udgaonkar, *Annu. Rev. Biophys. Biomol. Struct.* **37**, 489 (2008).

¹⁶ J. Kubelka, J. Hofrichter, and W. A. Eaton, *Curr. Opin. Struct. Biol.* **14**, 76 (2004).

¹⁷ M. Gruebele, *C. R. Seances Soc. Biol. Fil.* **328**, 701 (2005).

¹⁸ N. Go, *Annu. Rev. Biophys. Bioeng.* **12**, 183 (1983).

¹⁹ J. D. Bryngelson and P. G. Wolynes, *Proc. Natl. Acad. Sci. U.S.A.* **84**, 7524 (1987).

²⁰ H. S. Chung and A. Tokmakoff, *Proteins: Struct., Funct., Bioinf.* **72**, 474 (2008).

²¹ A. N. Naganathan, R. Perez-Jimenez, J. M. Sanchez-Ruiz, and V. Munoz, *Biochemistry* **44**, 7435 (2005).

²² M. Sadqi, D. Fushman, and V. Muñoz, *Nature (London)* **442**, 317 (2006).

²³ A. Fung, P. Li, R. Godoy-Ruiz, J. M. Sanchez-Ruiz, and V. Munoz, *J. Am. Chem. Soc.* **130**, 7489 (2008).

²⁴ A. N. Naganathan and V. Munoz, *Biochemistry* **47**, 6752 (2008).

²⁵ F. Liu and M. Gruebele, *J. Mol. Biol.* **370**, 574 (2007).

²⁶ H. Ma and M. Gruebele, *Proc. Natl. Acad. Sci. U.S.A.* **102**, 2283 (2005).

²⁷ F. Liu, D. Du, A. A. Fuller, J. Davoren, P. Wipf, J. Kelly, and M. Gruebele, *Proc. Natl. Acad. Sci. U.S.A.* **105**, 2369 (2008).

²⁸ W. Yang and M. Gruebele, *Biophys. J.* **87**, 596 (2004).

²⁹ Y. Zhu, D. O. V. Alonso, K. Maki, C.-Y. Huang, S. J. Lahr, V. Daggett, H. Roder, W. F. DeGrado, and F. Gai, *Proc. Natl. Acad. Sci. U.S.A.* **100**, 15486 (2003).

³⁰ M. Gruebele, *Proteins: Struct., Funct., Bioinf.* **70**, 1099 (2008).

³¹ R. Zwanzig, *Proc. Natl. Acad. Sci. U.S.A.* **85**, 2029 (1988).

³² S. T. R. Walsh, V. I. Sukharev, S. F. Betz, N. L. Vekshin, and W. F. DeGrado, *J. Mol. Biol.* **305**, 361 (2001).

³³ R. M. Ballew, J. Sabelko, and M. Gruebele, *Proc. Natl. Acad. Sci. U.S.A.* **93**, 5759 (1996).

³⁴ J. Ervin, J. Sabelko, and M. Gruebele, *J. Photochem. Photobiol., B* **54**, 1 (2000).

³⁵ H. Ma and M. Gruebele, *J. Comput. Chem.* **27**, 125 (2006).

³⁶ F. Liu and M. Gruebele, *Chem. Phys. Lett.* **461**, 1 (2008).

³⁷ G. Hummer, *New J. Phys.* **7**, 34 (2005).

³⁸ See EPAPS Document No. E-JCPSA6-130-040906 for additional thermodynamic data and the detailed functional form of the free energy surfaces used. For more information on EPAPS, see <http://www.aip.org/epaps/numbering.html>.

³⁹ W. Y. Yang and M. Gruebele, *J. Am. Chem. Soc.* **126**, 7758 (2004).

⁴⁰ D. M. Vu, E. S. Peterson, and B. B. Dyer, *J. Am. Chem. Soc.* **126**, 6546 (2004).

⁴¹ A. N. Naganathan, U. Doshi, and V. Munoz, *J. Am. Chem. Soc.* **129**, 5673 (2007).

⁴² Y. Xu, P. Purkayashita, and F. Gai, *J. Am. Chem. Soc.* **128**, 15836 (2006).

⁴³ J. W. Bryson, J. R. Desjarlais, T. M. Handel, and W. F. DeGrado, *Protein Sci.* **7**, 1404 (1998).

⁴⁴ S. T. Walsh, V. I. Sukharev, S. F. Betz, N. L. Vekshin, and W. F. DeGrado, *J. Mol. Biol.* **305**, 361 (2001).